ELSEVIER

11 December 1995

Physics Letters A 209 (1995) 69–77

PHYSICS LETTERS A

Electron beam and pulsed corona processing of carbon tetrachloride in atmospheric pressure gas streams

B.M. Penetrante [a], M.C. Hsiao [a], J.N. Bardsley [a], B.T. Merritt [a], G.E. Vogtlin [a], P.H. Wallman [a], A. Kuthi [b], C.P. Burkhart [b], J.R. Bayless [b]

[a] *Lawrence Livermore National Laboratory, Livermore, CA 94550, USA*
[b] *First Point Scientific, Inc., Agoura Hills, CA 91301, USA*

Received 17 August 1995; revised manuscript received 4 October 1995; accepted for publication 11 October 1995
Communicated by M. Porkolab

Abstract

Experimental results are presented on electron beam and pulsed corona processing of atmospheric-pressure gas streams containing dilute concentrations of carbon tetrachloride (CCl_4). Electron beam processing is remarkably more energy efficient than pulsed corona processing in decomposing CCl_4. The specific energy consumption in each reactor is consistent with dissociative electron attachment as the dominant decomposition pathway. The energy efficiency of the plasma process is insensitive to the gas temperature, at least up to 300°C. By doing the experiments using both dry air and N_2, the contribution of O radicals in the decomposition of CCl_4 is assessed. A discussion of the chemical kinetics starting from the initial decomposition of CCl_4 to the formation of products is presented.

1. Introduction

Non-thermal plasma processing is an emerging technology for the abatement of volatile organic compounds (VOCs) in atmospheric-pressure gas streams. Either electron beam irradiation or electrical discharge methods can produce these plasmas. The basic principle that these techniques have in common is to produce a plasma in which a majority of the electrical energy goes into the production of energetic electrons, rather than into gas heating. Through electron-impact dissociation and ionization of the background gas molecules, the energetic electrons produce free radicals and additional electrons which, in turn, oxidize or decompose the VOC molecules. The potential of electron beam and electrical discharge methods has been demonstrated for the decomposition of many types of VOCs [1]. Electrical discharge techniques can be implemented in many ways, depending on the electrode configuration and electrical power supply (pulsed, AC or DC). Among the more extensively investigated types of electrical discharge reactors are the pulsed corona and the dielectric-barrier discharge.

The use of an electron-beam generated plasma for the decomposition of carbon tetrachloride (CCl_4) in

---

[1] A collection of papers on various types of non-thermal plasma reactors being investigated for VOC abatement appears in Ref. [1].

SSDI 0375-9601(95)00789-X

dry and humid air streams was reported previously in Refs. [2] and [3]. The use of a dielectric-barrier discharge plasma for the decomposition of CCl_4 in dry and humid mixtures of 80% Ar + 20% O_2 was reported in Ref. [4]. In the present paper we report on non-thermal plasma processing of carbon tetrachloride using an electron beam reactor and a pulsed corona reactor. To the knowledge of the authors, this is the first comparison of the energy efficiency of electron beam and electrical discharge processing of CCl_4 under identical gas conditions. We observe that electron beam processing is remarkably more energy efficient than pulsed corona processing in decomposing CCl_4. The specific energy consumption in each reactor is consistent with dissociative electron attachment as the dominant decomposition pathway, as suggested in Refs. [2] and [3]. We also observe that the energy efficiency of the plasma process is insensitive to the gas temperature, at least up to 300°C. By doing the experiments using both dry air and N_2, we have been able to assess the contribution of O radicals in the decomposition of CCl_4. We discuss the chemical kinetics starting from the initial decomposition of CCl_4 to the formation of products.

2. Test facility

The electron beam reactor in our experiments used a cylindrical electron gun. This gun was designed to deliver a cylindrically symmetric electron beam that is projected radially inward through a 5 cm wide annular window into a 17 cm diameter flow duct. An electron beam of 125 keV energy was introduced into the reaction chamber through a 0.7 mil thick titanium window. The electron beam current was produced from a low-pressure helium plasma in an annular vacuum chamber surrounding the flow duct. A combined experimental and computer modeling approach was used to estimate the electron beam power deposition into the reaction chamber. Two sets of beam current measurements were performed to accurately determine the current delivery efficiency of the cylindrical electron gun. In one set a small area probe provided azimuthal and axial resolution of the beam current density in the absence of the vacuum window. In the other set a large area probe collected the entire beam in the presence of the vacuum window. Electron transport through the window and deposition into the probe was modeled with thc 2-D CYLTRAN code to correct for electron energy losses in the window, the probe view factor to the scattered electron distribution, and secondary electron emission from the probe surface. This 2-D Monte Carlo simulation was used to determine the dose distribution in the cylindrical duct as a function of the electron beam energy, window design (material and thickness) and duct diameter. The small probe results were averaged azimuthally and axially, and the averaged signal was corrected for geometrical effects for comparison with the data obtained with the large area probe. The two measurements agreed to better than 6%, thus indicating an accurate measure of the current delivery efficiency from which the dose in the process gas was determined. The electron reflection from the 0.7 mil titanium window is around 21%, while the electron absorption by the window is around 22%. The transmission efficiency of the beam current is thus 57%.

The pulsed corona reactor used in our experiment consisted of a wire (1.5 mm diameter) in a 300 mm long metal pipe with an inner diameter of 60 mm. The reactor was driven by a pulsed high-voltage power supply. This power supply was a magnetic pulse compression system capable of delivering up to 15–35 kV output in 100 ns FWHM pulses at repetition rates from 100 Hz to 1 kHz. We measure the total current which contains both the discharge current and the current associated with charging the capacitance of the reactor. A computer data acquisition system reads the voltage and current profiles and integrates the product of the voltage and discharge current over the pulse duration to yield the pulse energy. The determination of the power input to the gas corrects for the capacitive current. In these experiments the power input to the processor was varied by changing either the pulse energy or pulse repetition frequency. The important control parameter was the energy density input, which is the ratio of power input into the gas to the gas flow rate. For the same energy density input, either method produced almost identical results. The gas mixtures were set with mass flow controllers. The gas and processor temperatures were maintained at a temperature that can be controlled from 25°C to 300°C. The experimental apparatus has been described in detail in Refs. [5] and [6].

All the plasma processing experiments were performed in a flow-through configuration at atmospheric pressure. To characterize the energy consumption of the process for each VOC, the composition of the effluent gas was recorded as a function of the input energy density. The input energy density, in units of joules per standard liter (J/L), is the ratio of the power (deposited into the gas) to gas flow rate at standard conditions (25°C and 1 atm). The amount of VOC was quantified using an FTIR analyzer and a gas chromatograph/mass spectrometer.

3. Processing in dry air

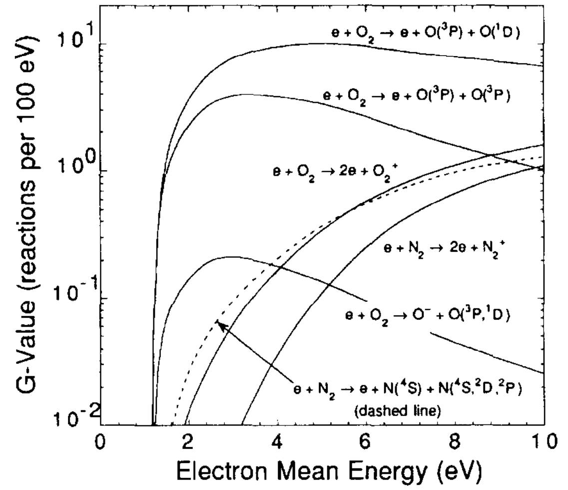

Fig. 1. Calculated G-values (number of reactions per 100 eV of input energy) for dissociation and ionization processes in dry air, shown as functions of the electron mean energy in a discharge plasma.

Table 1
Calculated G-values (number of reactions per 100 eV of input energy) for dissociation processes in dry air using an electron beam and an electrical discharge reactor

Reaction	Electron beam	Discharge
$e+N_2 \to e+N(^4S)+N(^4S,^2D,^2P)$	1.2	0.17
$e+O_2 \to e+O(^3P)+O(^3P)$	1.3	4.0
$e+O_2 \to e+O(^3P)+O(^1D)$	2.65	10.0
$e+O_2 \to O^- +O(^3P,^1D)$	0.11	0.19

In non-thermal plasma processing of a mixture containing very dilute concentrations of CCl_4, the input electrical energy is dissipated by the primary electrons mostly in interactions with the background gas molecules. The energetic primary electrons produce free radicals and electron–ion pairs through electron-impact dissociation and ionization. In a dry air mixture, electron-impact dissociation of molecular oxygen [7–9] produces the ground state atomic oxygen $O(^3P)$ and excited atomic oxygen $O(^1D)$,

$$e + O_2 \to e + O(^3P) + O(^3P) \qquad (1a)$$

$$e + O_2 \to e + O(^3P) + O(^1D) \qquad (1b)$$

In addition, with energetic electrons, $O(^3P)$ and $O(^1D)$ can be produced via two-body dissociative attachment [10]

$$e + O_2 \to O^- + O(^3P,\ ^1D) \qquad (1c)$$

In discharge processing, the rate coefficients for electron-impact dissociation reactions strongly depend on the electron mean energy in the discharge plasma. In pulsed corona and dielectric-barrier discharge reactors, the non-thermal plasma is produced through the formation of statistically distributed microdischarges. The electrons dissociate and ionize the background gas molecules within nanoseconds in the narrow channel formed by each microdischarge. The electron energy distribution in the plasma is complicated because the electric field is strongly non-uniform (e.g. because of strong space-charge field effects) and time dependent. However, most of the species responsible for the chemical processing are generated in the microdischarge channels already established during the main current flow. In each microdischarge column, the electrons acquire a drift velocity, v_d, and an average energy corresponding to an effective E/n, i.e., the value of the electric field E divided by the total gas density n. The efficiency for a particular electron-impact process can be expressed in terms of the G-value (number of dissociation or ionization reactions per 100 eV of input energy) defined as

$$G_{\text{value}} = \frac{100\,k/}{v_d E/n}, \qquad (2)$$

where k is the rate coefficient (cm^3/molecule s). The rate coefficient k represents the number of reactions in a unit volume per unit time. The quantity $v_d E/n$ represents the amount of energy expended by the electrons in a unit volume per unit time. In Fig. 1 the calculated G-values for various electron-impact dissociation and ionization processes in dry air are shown as functions of the electron mean energy in the discharge plasma [11]. The main contribution to O radical production comes from the dissociation reactions (1a) and (1b).

Under most conditions encountered in pulsed corona or dielectric-barrier discharge processing, the effective E/n is close to the value for breakdown (Paschen field) [9,11]. For dry air, the effective E/n is around 130 Td (1 Td $= 10^{-17}$ V cm^2), which corresponds to an electron mean energy of about 4 eV. Table 1 shows a comparison of the calculated G-values for dissociation processes in dry air using an electron beam and a discharge reactor. Discharge plasma conditions are optimum for the dissociation of O_2. The production of O radicals is higher in a pulsed corona reactor compared to that in an electron beam reactor.

The O radicals can dissociate CCl_4 into ClO and CCl_3 [12-14],

$$O(^3P) + CCl_4 \rightarrow ClO + CCl_3, \quad (3a)$$

$$O(^1D) + CCl_4 \rightarrow ClO + CCl_3. \quad (3b)$$

Another mechanism for the dissociation of CCl_4 is through the secondary electrons. Electron-ion pairs are produced through various electron-impact ionization processes [15,16],

$$e + N_2 \rightarrow 2e + N_2^+, \quad (4)$$

$$e + N_2 \rightarrow 2e + N(^4S) + N^+, \quad (5)$$

$$e + N_2 \rightarrow 2e + N(^2D) + N^+, \quad (6)$$

$$e + O_2 \rightarrow 2e + O_2^+, \quad (7)$$

$$e + O_2 \rightarrow 2e + O(^1D) + O^+. \quad (8)$$

The secondary electrons can dissociate CCl_4 via dissociative electron attachment [17,18] to produce CCl_3 and a negative ion Cl^-,

$$e + CCl_4 \rightarrow CCl_3 + Cl^-. \quad (9)$$

The rate coefficient for reaction (9) is on the order of 10^{-7} cm^3/molecule s [17,18]. The rate coefficient for reaction (3a) is less than 10^{-14} cm^3/molecule s [12], while that for reaction (3b) is around 10^{-10} cm^3/molecule s [13,14]. Table 2 shows a comparison of the calculated G-values for ionization processes in dry air using an electron beam and a discharge reactor. The production of electron-ion pairs is higher in an electron beam reactor compared to that in a pulsed corona reactor. An examination of the G-values shown in Tables 1 and 2 indicates that dissociative electron attachment will dominate the initial decomposition of CCl_4 for both electron beam and electrical discharge reactor conditions.

Table 2

Calculated G-values (number of reactions per 100 eV of input energy) for ionization processes in dry air using an electron beam and an electrical discharge reactor

Reaction	Electron beam	Discharge
$e + N_2 \rightarrow 2e + N(^4S,^2D) + N^+$	0.69	$< 10^{-6}$
$e + N_2 \rightarrow 2e + N_2^+$	2.27	0.044
$e + O_2 \rightarrow 2e + O_2^+$	2.07	0.17
$e + O_2 \rightarrow 2e + O(^1D) + O^+$	1.23	0.0016

The charge exchange reaction of positive ions, such as N_2^+, with the background O_2 is fast, resulting in mostly O_2^+ ions [19],

$$N_2^+ + O_2 \rightarrow N_2 + O_2^+. \quad (10)$$

The positive ions react with Cl^- through the ion-ion neutralization reaction to produce Cl and O radicals,

$$Cl^- + O_2^+ \rightarrow Cl + 2O. \quad (11)$$

In the absence of scavenging reactions for CCl_3, the input energy would be wasted because Cl and CCl_3 would simply recombine quickly to reform the original pollutant [20,21],

$$Cl + CCl_3 + M \rightarrow CCl_4 + M. \quad (12)$$

Fortunately, the presence of O_2 scavenges the CCl_3 through the fast reaction [22,23],

$$CCl_3 + O_2 + M \rightarrow CCl_3O_2 + M. \quad (13)$$

The CCl_3O_2 species undergoes a chain reaction involving the Cl radical and produces phosgene ($COCl_2$) as one of the main organic products [24,14],

$$Cl + CCl_3O_2 \rightarrow CCl_3O + ClO, \quad (14)$$

$$CCl_3O \rightarrow COCl_2 + Cl. \quad (15)$$

The ClO species produces additional Cl radicals through a reaction with the O radicals [25,14],

$$O + ClO \rightarrow Cl + O_2. \tag{16}$$

The other major product is Cl_2 which is formed by the reaction [25],

$$Cl + Cl + M \rightarrow Cl_2 + M. \tag{17}$$

The CCl_3 species from reaction (9) can also be scavenged by O [26],

$$CCl_3 + O \rightarrow COCl_2 + Cl, \tag{18}$$

and by N [27],

$$CCl_3 + N \rightarrow ClCN + 2Cl. \tag{19}$$

The apparent two-body rate constant for scavenging reaction (13) is $1.4 \times 10^{-9}\ T^{-1.1}$ (cm^3/molecule s). The rate constants are 4.2×10^{-11} and 1.7×10^{-11} (cm^3/molecule s) for scavenging reactions (18) and (19), respectively. Because of the much larger density of O_2 compared to O or N, the scavenging of CCl_3 by reactions (18) and (19) are therefore negligible compared to reaction (13) during processing in dry air.

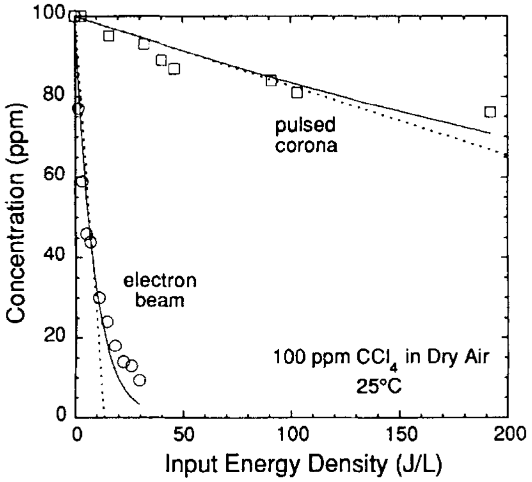

Fig. 2. Comparison between electron beam and pulsed corona processing of 100 ppm of carbon tetrachloride in dry air at 25°C. The solid lines are fits to the experimental data points (circles and squares) using the expression $[X] = [X]_0 \exp(-E/\beta)$. The dotted lines are results of chemical kinetics calculations using the ionization G-values in Table 1.

Fig. 2 shows the results of experiments on electron beam and pulsed corona processing of 100 ppm of CCl_4 in dry air (20% O_2, 80% N_2) at 25°C. The solid lines are fits to the experimental data points using the expression $[X] = [X]_0 \exp(-E/\beta)$, where $[X]_0$ is the initial CCl_4 concentration, E is the input energy density, and β is the exponential-folding factor. This empirical expression has been suggested by Rosocha et al. [4] as a figure of merit for comparing energy efficiencies for destruction. The exponential-folding factors for electron beam and pulsed corona processing are 9 and 555 J/L, respectively.

An analysis of the rates of the reactions discussed above suggests that the rate limiting step in the decomposition of CCl_4 is determined by the dissociative attachment of CCl_4 to the thermalized electrons in the created plasma. The specific energy consumption for CCl_4 removal is therefore determined by the specific energy consumption (or G-value) for creating electron–ion pairs. Table 2 shows the calculated G-values for the ionization processes (4)–(8). For electron beam processing of dry air, the ionization G-value corresponds to a specific energy consumption of 33 eV per electron–ion pair produced. For pulsed corona processing, we calculate a specific energy consumption of around 1400 eV per electron–ion pair, assuming an effective electron mean energy of 4 eV in the discharge plasma. The results of our chemical kinetics calculations are shown as dotted lines in Fig. 2. To first order, the calculated specific energy consumption for electron–ion pair production agrees very well with our experimentally observed specific energy consumption for CCl_4 decomposition. The results shown in Fig. 2 demonstrate that for VOCs requiring copious amounts of electrons for decomposition, electron beam processing is much more energy efficient than electrical discharge processing.

After the concentration of CCl_4 has decreased to a few tens of ppm, the three-body attachment of thermal electrons to oxygen molecules [10],

$$e + O_2 + O_2 \rightarrow O_2^- + O_2, \tag{20}$$

$$e + O_2 + N_2 \rightarrow O_2^- + N_2, \tag{21}$$

becomes a significant electron loss pathway compared to reaction (9). The rate constants for reactions

(20) and (21) are $k_{(20)} = 2.5 \times 10^{-30}$ and $k_{(21)} = 0.16 \times 10^{-30}$ cm^6/s, respectively. The attachment frequency of thermal electrons to O_2 in dry air at atmospheric pressure is thus

$$\nu_{O_2} = k_{(20)}[O_2]^2 + k_{(21)}[N_2][O_2] \approx 0.8 \times 10^8 \text{ s}^{-1}.$$

The attachment rate coefficient for thermal electrons to CCl_4 is $k_{(9)} = 4 \times 10^{-7}$ cm^3/s. For 100 ppm CCl_4, the attachment frequency to CCl_4 is thus

$$\nu_{CCl_4} = k_{(9)}[CCl_4] \approx 10^9 \text{ s}^{-1}.$$

When the concentration of CCl_4 is down to around 10 ppm, the electrons will attach to oxygen molecules as frequently as to CCl_4 molecules.

Although the dominant pathway (dissociative electron attachment) for the initial decomposition of CCl_4 is the same in electron beam and pulsed corona processing, the composition of the final products are not the same. In pulsed corona processing, a larger amount of O radicals is produced relative to the amount of electrons. Even though these O radicals contribute only a small fraction to the initial decomposition of CCl_4, they do interact significantly with phosgene to change the composition of the final products [12,28],

$$O + COCl_2 \rightarrow ClO + COCl, \tag{22}$$

$$COCl + M \rightarrow CO + Cl + M, \tag{23}$$

$$O + COCl \rightarrow CO_2 + Cl. \tag{24}$$

Our model for the decomposition mechanism predicts a difference in product yields between electron beam and pulsed corona processing at the minimum energy required for near complete decomposition of CCl_4. For around 95% decomposition of 100 ppm CCl_4 in dry air by electron beam processing, the final products consist of around 100 ppm Cl_2 and 100 ppm $COCl_2$. For the same level decomposition of 100 ppm CCl_4 in dry air by pulsed corona processing, the final products consist of around 160 ppm Cl_2, 40 ppm $COCl_2$, 50 ppm CO and 10 ppm CO_2. Of course, with excessive energy deposition all the $COCl_2$ would eventually be converted into CO_x and Cl_2. However, as noted in Refs. [29] and [30], the Cl_2 and $COCl_2$ products can be easily removed from the gas stream; e.g. they dissolve and/or dissociate in aqueous solutions and combine with $NaHCO_3$ in a scrubber solution to form NaCl [30].

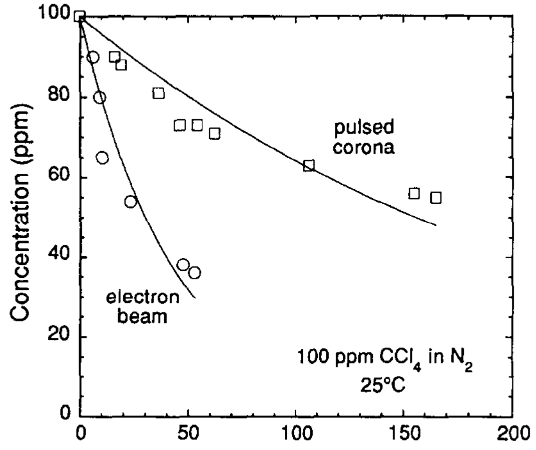

Fig. 3. Comparison between electron beam and pulsed corona processing of 100 ppm of carbon tetrachloride in N_2 at 25°C. The solid lines are fits to the experimental data points using the expression $[X] = [X]_0 \exp(-E/\beta)$.

4. Processing in N_2

In pure N_2 one might expect Cl and CCl_3 to simply recombine back to CCl_4 because of the absence of the scavenging reaction (13). Fortunately, electron-impact dissociation of N_2 produces N atoms that serve to scavenge CCl_3 [27] through reaction (19). The specific energy consumption for CCl_4 decomposition is then determined by the energy cost for dissociating N_2 and the rate of reaction (19) relative to reaction (12).

Fig. 3 shows the results of experiments on electron beam and pulsed corona processing of 100 ppm of CCl_4 in N_2 at 25°C. The exponential-folding factors for electron beam and pulsed corona processing are 44 and 224 J/L, respectively.

For electron beam processing in N_2, it costs 33 eV to produce an electron and around 40 eV to produce an N atom [31]. Each electron will attach to

CCl_4 and produce Cl. For the same energy input, there will therefore be approximately the same number of N and Cl atoms produced. The rate coefficient for reaction (12) is around 5×10^{-11} cm^3/molecule s [20], while that for reaction (19) is estimated to be around 1.7×10^{-11} cm^3/molecule s [27]. The CCl_3 species is therefore about three times more likely to recombine with Cl than to be scavenged by N. This means that the specific energy consumption for electron beam decomposition of CCl_4 in N_2 should be around three to four times higher compared to that in dry air. This argument is consistent with the experimental result shown in Fig. 3. For pulsed corona processing in N_2, it costs around 1400 eV to produce an electron and only about 240 eV to produce an N atom [31]. The specific energy consumption for pulsed corona processing of CCl_4 in N_2 is thus also limited by the energy cost for producing electron–ion pairs, similar to that in dry air.

The experimental result in Fig. 3 shows that pulsed corona processing of CCl_4 in N_2 is more energy efficient compared to that in dry air. This observation probably indicates that the effective electron mean energy of the discharge plasma in N_2 is higher compared to that in dry air. As discussed in the previous section, the electron mean energy in a pulsed corona or dielectric-barrier discharge is determined by an effective electric field that has a value close the breakdown field [9,11]. The breakdown field in N_2 is only slightly higher compared to that in dry air. However, the G-value for ionization is very sensitive to the electron mean energy, as shown in Fig. 1. A slightly higher electron mean energy means that more secondary electrons are produced, which in turn means a higher CCl_4 destruction efficiency.

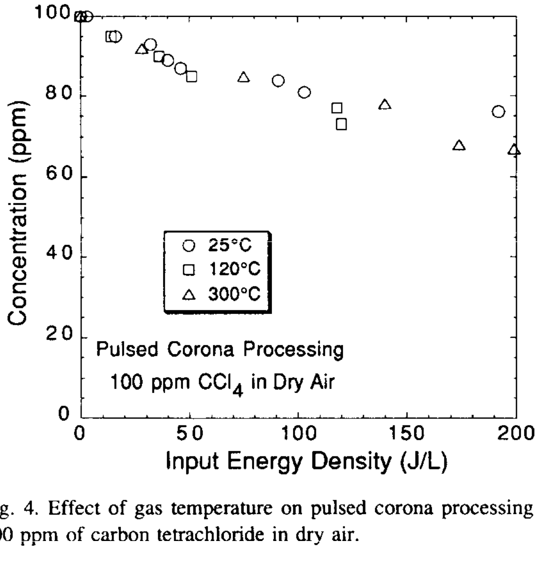

Fig. 4. Effect of gas temperature on pulsed corona processing of 100 ppm of carbon tetrachloride in dry air.

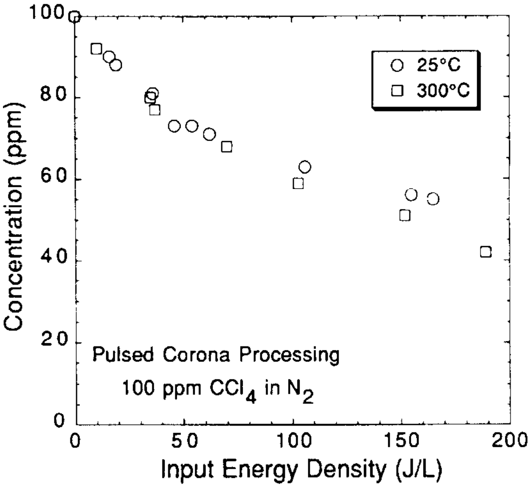

Fig. 5. Effect of gas temperature on pulsed corona processing of 100 ppm of carbon tetrachloride in N_2.

5. Effect of gas temperature

Fig. 4 shows the results of experiments on pulsed corona processing of 100 ppm of CCl_4 in dry air at 25°, 120°, and 300°C. Even though the decomposition reaction (3) of CCl_4 by the O radicals is gas temperature dependent [12], the rate limiting step in the decomposition of CCl_4 is determined by dissociative electron attachment. The energy consumption is therefore determined by the efficiency for producing electrons, and we would not expect any significant change in the energy consumption for CCl_4 decomposition as the gas temperature is varied. This explanation is consistent with the experimental results shown in Fig. 4. Fig. 5 shows the results of experiments on pulsed corona processing of 100 ppm of CCl_4 in N_2 at 25° and 300°C. Again in this mixture, the decomposition of CCl_4 is determined by the efficiency for producing electrons, and we would not expect any significant change in the energy consumption as the gas temperature is varied.

6. Conclusions

We have presented experimental results on electron beam and pulsed corona processing of atmospheric-pressure gas streams containing dilute concentrations of CCl_4. To our knowledge, this is the first comparison of the energy efficiency of electron beam and electrical discharge processing of CCl_4 under identical gas conditions. Our results show that electron beam processing is remarkably more energy efficient than pulsed corona processing in decomposing CCl_4. The specific energy consumption in each reactor is consistent with dissociative electron attachment as the dominant decomposition pathway. Our results demonstrate that for VOCs requiring copious amounts of electrons or ions for decomposition, electron beam processing is much more energy efficient than electrical discharge processing. The energy efficiency of the plasma process is insensitive to the gas temperature, at least up to 300°C. We also assessed the contribution of O radicals in the decomposition of CCl_4. In electron beam processing of CCl_4 in dry air, the final products consist of approximately equal amounts of Cl_2 and $COCl_2$. In pulsed corona processing of CCl_4 in dry air, the O radicals interact with $COCl_2$ and produce CO as another major product, in addition to Cl_2, $COCl_2$ and CO_2.

Acknowledgements

This work was performed in part at Lawrence Livermore National Laboratory under the auspices of the U.S. Department of Energy under Contract Number W-7405-ENG-48, with support from the Advanced Energy Projects Division of the Office of Energy Research and a Cooperative Research and Development Agreement with Cummins Engine Company. The electron beam processing equipment was developed under a National Science Foundation SBIR grant, Contract Number III-9122767.

References

[1] B.M. Penetrante and S.E. Schultheis, eds., Non-thermal plasma techniques for pollution control: Part A – Overview, fundamentals and supporting technologies, Part B – Electron beam and electrical discharge processing (Springer, Berlin, 1993).

[2] L. Bromberg, D.R. Cohn, M. Koch, R.M. Patrick and P. Thomas, Phys. Lett. A 173 (1993) 293.

[3] M. Koch, D.R. Cohn, R.M. Patrick, M.P. Schuetze, L. Bromberg, D. Reilly and P. Thomas, Phys. Lett. A 184 109 (1993).

[4] L.A. Rosocha, G.K. Anderson, L.A. Bechtold, J.J. Coogan, H.G. Heck, M. Kang, W.H. McCulla, R.A. Tennant and P.J. Wantuck, in: Non-Thermal plasma techniques for pollution control: Part B – Electron beam and electrical discharge processing, eds. B.M. Penetrante and S.E. Schultheis (Springer, Berlin, 1993) pp. 281–308.

[5] M.C. Hsiao, B.T. Merritt, B.M. Penetrante, G.E. Vogtlin and P.H. Wallman, J. Appl. Phys. 78, (1995) 3451.

[6] B.M. Penetrante, M.C. Hsiao, B.T. Merritt, G.E. Vogtlin and P.H. Wallman, IEEE Trans. Plasma Sci. 23 (1995), to be published.

[7] E.C. Zipf, in: Electron – molecule interactions and their applications, ed. L. Christophorou, Vol. 1 (Academic Press, New York, 1984) pp. 335–401.

[8] P.C. Cosby, J. Chem. Phys. 98 (1993) 9560.

[9] B. Eliasson and U. Kogelschatz, J. Phys. B, 19, (1986) 1241.

[10] L.M. Chanin, A.V. Phelps and M.A. Biondi, Phys. Rev. 128, (1962) 219.

[11] B.M. Penetrante, in: Non-thermal plasma techniques for pollution control – Part A: Overview, fundamentals and supporting technologies, eds. B.M. Penetrante and S.E. Schultheis (Springer, Verlag, Berlin, 1993) pp. 65–90.

[12] J.T. Herron, J. Phys. Chem. Ref. Data 17 (1988) 967.

[13] J.A. Davidson, H.I. Schiff, T.J. Brown, C.J. Howard, J. Chem. Phys. 69 (1978) 4277.

[14] R. Atkinson, D.L. Baulch, R.A. Cox, R.F. Hampson Jr., J.A. Kerr and J. Troe, J. Phys. Chem. Ref. Data 21 (1992) 1125–1568.

[15] Y. Itikawa, M. Hayashi, A. Ichimura, K. Onda, D. Sakimoto, K. Takayanagi, M. Nakamura, H. Nishimura and T. Takayanagi, J. Phys. Chem. Ref. Data 15 (1986) 985.

[16] Y. Itikawa, A. Ichimura, K. Ondaz, K. Sakimoto, K. Takayanagi, Y. Hatano, M. Hayashi, H. Nishimura and S. Tsurubuchi, J. Phys. Chem. Ref. Data 18 (1989) 23.

[17] A.A. Christodoulides and L.G. Christophorou, J. Chem. Phys. 54 (1971) 4691.

[18] J.A. Ayala, W.E. Wentworth and E.C.M. Chen, J. Phys. Chem. 85 (1981) 3989.

[19] D.L. Albritton, At. Data Nucl. Data Tables 22 (1978) 1.

[20] F. Danis, F. Caralp, B. Veyret, H. Loirat and R. Lesclaux, Int. J. Chem. Kinet. 21 (1989) 715.

[21] T. Ellermann, Chem. Phys. Lett. 189 (1992) 175.

[22] F. Danis, F. Caralp, M.T. Rayez and R. Lesclaux, J. Phys. Chem. 95 (1991) 7300.

[23] F.F. Fenter, P.D. Lightfoot, J.T. Niiranen and D. Gutman, J. Phys. Chem. 97 (1993) 313.

[24] J.J. Russell, J.A. Seetula, D. Gutman, F. Danis, F. Caralp, P.D. Lightfoot, R. Lesclaux, C.F. Melius and S.M. Senkan, J. Phys. Chem. 94 (1990) 3277.

[25] D.L. Baulch, J. Duxbury, S.J. Grant and D.C. Montague, J. Phys. Chem. Ref. Data 10, Suppl. 1 (1981) 1.

[26] J.T. Herron, J. Phys. Chem. Ref. Data 17 (1988) 967.

[27] S.C. Jeoung, K.Y. Choo and S.W. Benson, J. Phys. Chem. 95 (1991) 7282.

[28] W.-D. Chang and S.M. Senkan, Environ. Sci. Tech. 23 (1989) 442.

[29] D. Evans, L.A. Rosocha, G.K. Anderson, J.J. Coogan and M.J. Kushner, J. Appl. Phys. 74 (1993) 5378.

[30] R.M. Patrick and K. Hadidi, An electron beam plasma system for halogenated hydrocarbon vapor destruction, Preprint No. 95-WP77B.04, 88th Annual Meeting & Exhibition of the Air & Waste Management Association, San Antonio, TX, 18–23 June 1995.

[31] B.M. Penetrante, M.C. Hsiao, B.T. Merritt, G.E. Vogtlin, P.H. Wallman, A. Kuthi, C.P. Burkhart and J.R. Bayless, Appl. Phys. Lett., in press.